Available online at www.sciencedirect.com
ScienceDirect
Ceramics International 35 (2009) 2087–2091
CERAMICS INTERNATIONAL
www.elsevier.com/locate/ceramint

Short communication

Characterization of $CoWO_4$ nano-particles produced using the spray pyrolysis

Somchai Thongtem [a,*], Surangkana Wannapop [a], Titipun Thongtem [b]

[a] *Department of Physics, Faculty of Science, Chiang Mai University, Chiang Mai 50200, Thailand*
[b] *Department of Chemistry, Faculty of Science, Chiang Mai University, Chiang Mai 50200, Thailand*

Received 9 July 2008; received in revised form 3 October 2008; accepted 6 November 2008
Available online 9 December 2008

Abstract

$CoWO_4$ nano-particles were produced by spraying the solution containing $CoCl_2{\cdot}6H_2O$ and $Na_2WO_4{\cdot}2H_2O$ on glass slides at 250–450 °C. XRD, SAED, TEM, HRTEM and AFM revealed the presence of $CoWO_4$ nano-particles with their crystallographic planes aligning in systematic array. Raman spectra provide evidence of the wolframite structure, corresponding to the product phase. Their photoluminescence (PL) emissions show the narrow central peaks of the same spectral region at 411–419 nm.

Keywords: Spray pyrolysis; $CoWO_4$; Nano-particles

1. Introduction

Naturally, wolframite and scheelite are the majorities of tungsten ores formed on earth [1]. Their structures are controlled by cationic radii. Small radii (<0.077 nm) are in favor of forming wolframite structure, but large radii (>0.099 nm) favor scheelite structure [2,3]. Each of the tungsten atoms is surrounded by six oxygen atoms for wolframite [4], and by four oxygen atoms for scheelite [5]. The metal tungstates have very attractive properties in scintillation, electro-optics and microwave applications [1,4,6]. There are a number of methods used to prepare nano-structured tungstates, such as microwave-assisted synthesis [2,7], hydrothermal and solvothermal processes [3,6,8–10] and sonochemistry [11].

2. Experimental

For the present research, each 0.2 mol of $CoCl_2{\cdot}6H_2O$ and $Na_2WO_4{\cdot}2H_2O$ was dissolved in 25 ml de-ionized water and mixed. The mixture was stirred for 10 min and sprayed on glass slides 10 times in the temperature range 250–450 °C. The slides were kept at constant temperatures for 10 h, and removed from the furnace. No other additives were used in the process. It is simple and easy to handle, and more economical to process in large scale. The products were washed with de-ionized water and 95% ethanol, dried at 60 °C for 10 h and intensively characterized.

3. Results and discussion

Comparing XRD spectra (Fig. 1a) with that of the JCPDS software (reference code: 15-0867) [12], the products were $CoWO_4$ with monoclinic crystal system and P2/a space group. The phase has wolframite structure [2,3,13]. During characterization, X-ray beam reflected and diffracted with the crystalline products and sharp spectra were produced. Their strongest

* Corresponding author.
E-mail addresses: schthongtem@yahoo.com, sthongtem@hotmail.com (S. Thongtem).

0272-8842/$34.00
doi:10.1016/j.ceramint.2008.11.014

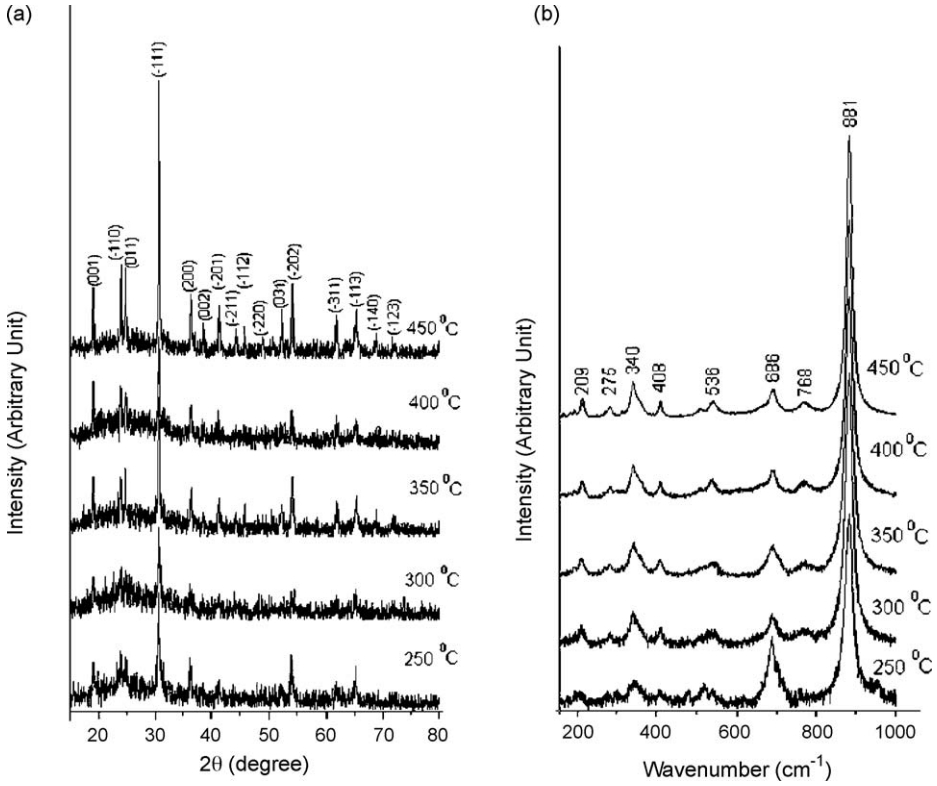

Fig. 1. (a) XRD and (b) Raman spectra of the products produced at different temperatures.

intensity peaks are at $2\theta = 30.6^\circ$ and diffracted from (−1 1 1) planes of the products. No other characteristic peaks of impurities were detected showing that the products are at a pure phase. XRD intensities were increased with the increase in the test temperatures which can play the role in arranging atoms in systematic order. Their crystallite sizes were enlarged as well. At 450 °C, XRD peaks have the strongest intensities and the crystallite sizes are the largest.

Raman spectra (Fig. 1b) of the wolframite structured products compose of a strong band at 881 cm^{-1} and a weak band at 768 cm^{-1}. They were specified as symmetric and asymmetric stretching vibrations of terminal W=O bonds, respectively [13]. The weak bands at 686 and 536 cm^{-1} are caused by the asymmetric and symmetric stretching of O–W–O bridges of $(W_2O_4)_n$ polymeric chain. Those at 408 and 340 cm^{-1} are tentatively specified as the in-plane deformation and rotation of W–O bonds (terminal and bridging), respectively. Weak band at 275 cm^{-1} is caused by Co–O stretching. The 209 cm^{-1} band is likely to be out-of-plane vibration [13]. The more Raman wavenumber of the atomic vibration does, the more the product structure distorts, and the opposite is also true [8].

TEM images (Fig. 2a–c) show a number of nano-particles influenced by test temperatures. Diameters (D) of 300 nano-particles at different temperatures were measured [14], and are shown in Fig. 3a–e. The products are composed of a number of nano-particles with different sizes. Their distributions are very close to the normal curves. The average sizes are in the ranges 16.25–25.23, 17.03–25.27, 22.65–42.59, 40.34–61.50 and 46.81–68.27 nm at 250, 300, 350, 400 and 450 °C, respectively. The values of log(D) and T^{-1} (Fig. 3f) matched very well with the Arrhenius-type equation [15],

$$\log D = 3.06 - \frac{946.21}{T}.$$

It shows that particle sizes increased monotonically with the increase in test temperature. It was assumed that heat capacity of formation of the nano-particles is constant with temperature. Calculated activation energy is 1.306×10^{-20} J·(particle)$^{-1}$, which is the energy consumption for every particle formed in the present process. Particle shape and size influence the PL as well. During the process, growth rates of the particles were very low. A number of nano-sized particles formed. HRTEM image (Fig. 2d) shows that a number of (0 0 2) lattice planes are in systematic array. Each grain is composed of atomic planes in the same direction, and corresponds to a single crystal. SAED patterns (Fig. 2a–c) show a number of random and continuous bright spots. They are so close that they form fully concentric rings. These indicate that the products consist of nano-sized crystals with different orientations. Calculated interplanar spaces

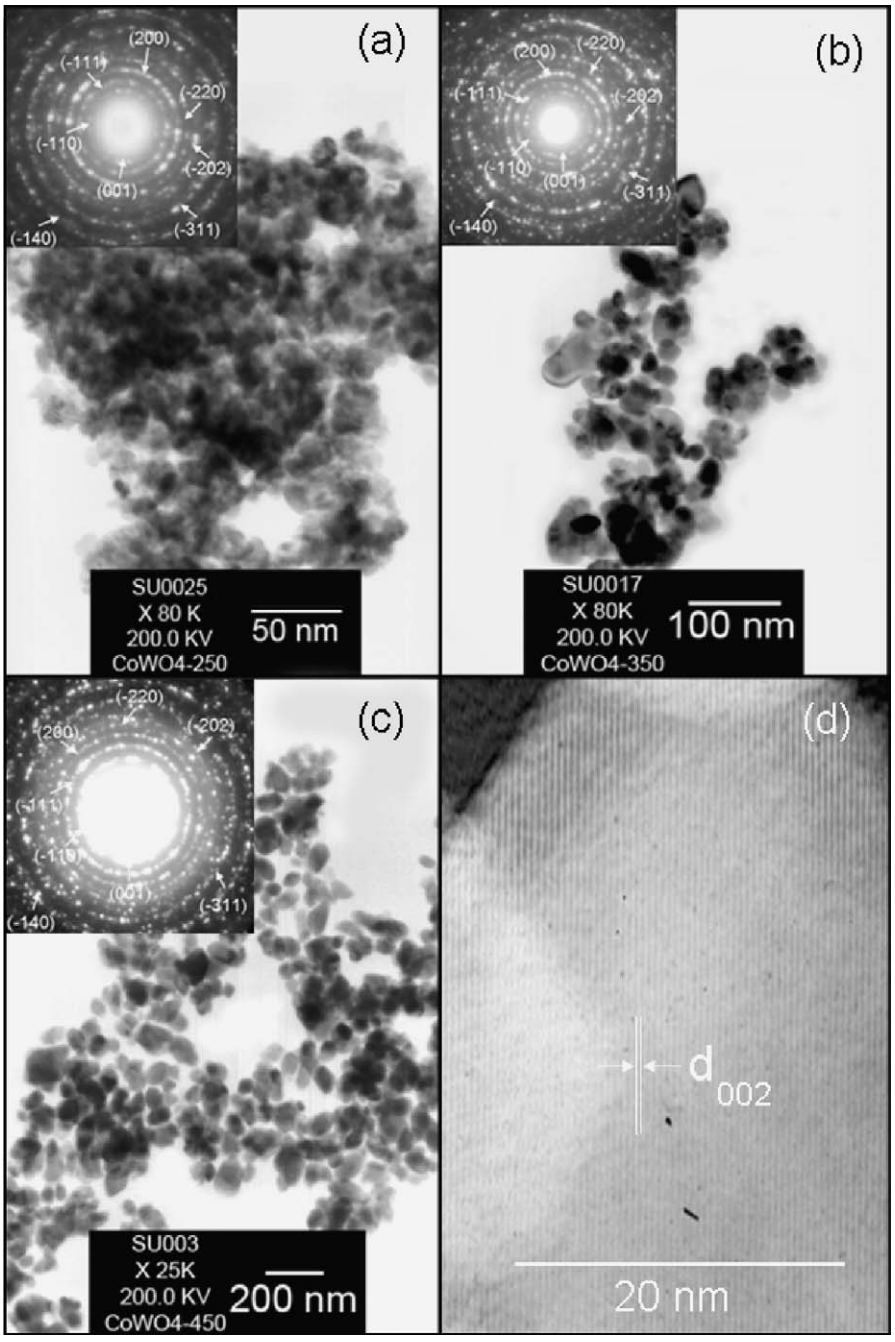

Fig. 2. (a–c) TEM images and SAED patterns of the products produced at 250, 350 and 450 °C, respectively. (d) HRTEM image of $CoWO_4$ produced at 450 °C.

[7] were compared with those of the JCPDS software [12]. They correspond to (0 0 1), (−1 1 0), (−1 1 1), (2 0 0), (−2 2 0), (−2 0 2), (−3 1 1) and (−1 4 0) planes of the crystals and were specified as $CoWO_4$.

The sprayed products on glass substrates at different temperatures were characterized using AFM. Fig. 4 shows the evolution of roughness with the test temperatures. The deposition did not form regular patterns. Surfaces of the substrates were very rough due to the deposited products. Their roughness at 250, 300, 350, 400 and 450 °C are 24.7, 45.8, 51.3, 95.5 and 106.9 nm, respectively. Roughness increased with the increase in test temperature. Nucleation and growth processes led to the irregular patterns on the substrates. Generally, vibration at high temperature was more violent than that at low temperature. Atoms and particles have more chance to arrange themselves in good order which is in favor with flat surface. For the present analysis, growth is the dominant process.

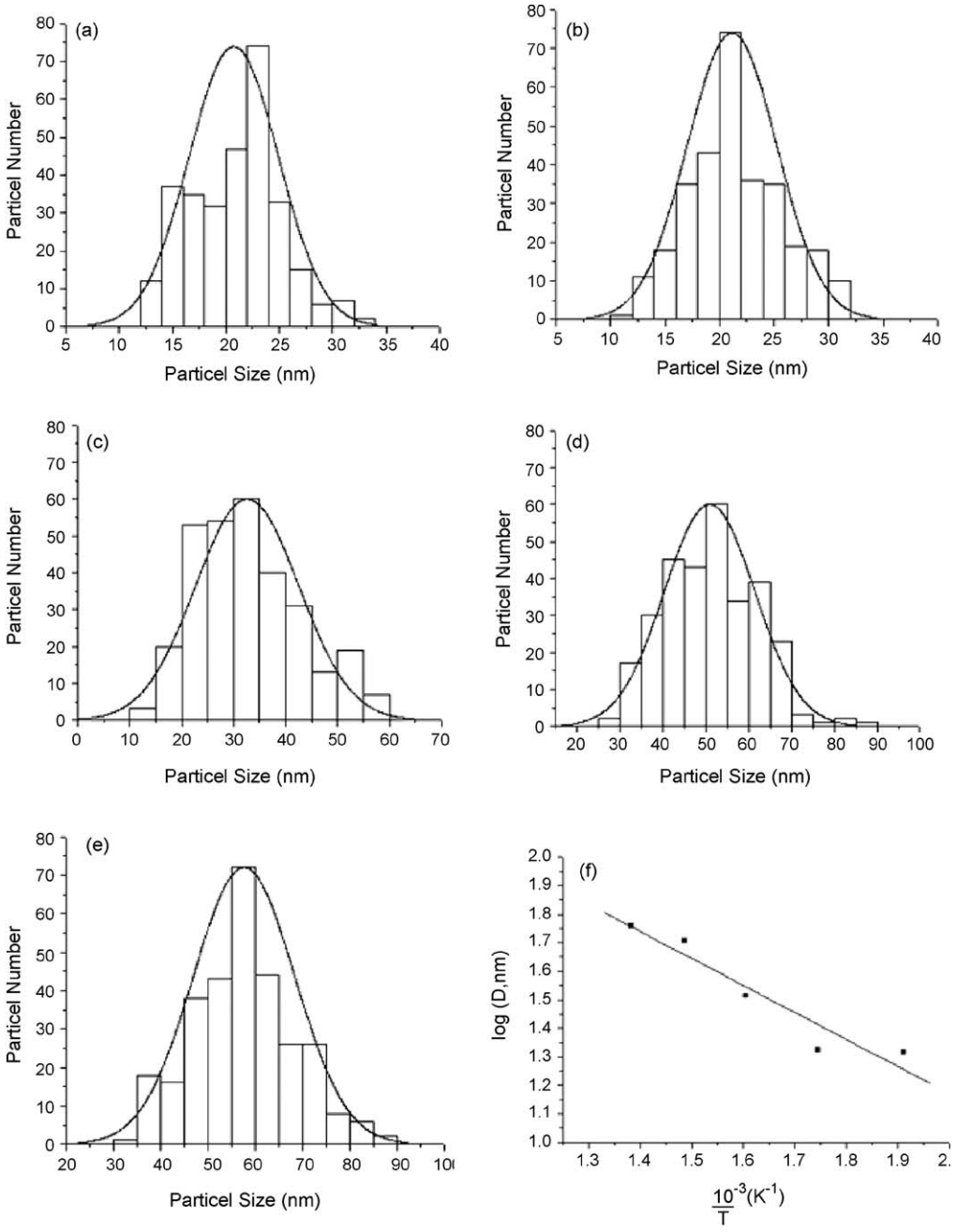

Fig. 3. (a–e) Particle size distributions of $CoWO_4$ produced at 250, 300, 350, 400 and 450 °C, respectively. (f) Particle size dependency on the temperature.

By using a 300 nm excitation wavelength, photoluminescence (PL) spectra (Fig. 5) show the narrow central (intrinsic) peaks with their surrounding shoulders [16–18]. The emission peaks are in the same spectral region at 411–419 nm although the products were produced at different temperatures. The intrinsic luminescence was caused by the annihilation of a self-trapped exciton, which formed excited $[WO_6]^{6-}$ complex [19]. It can be excited either in the excitonic absorption band or in the recombination process [19], due to the wolframite-structured products. The shoulders are from some defects and impurities. PL intensity is controlled by the number of charged transfers in the products. For present analysis, their intensities increased with the increase in test temperatures. It is the highest at 450 °C. Shapes, sizes, degree of crystallinity and others can play a role in emission as well.

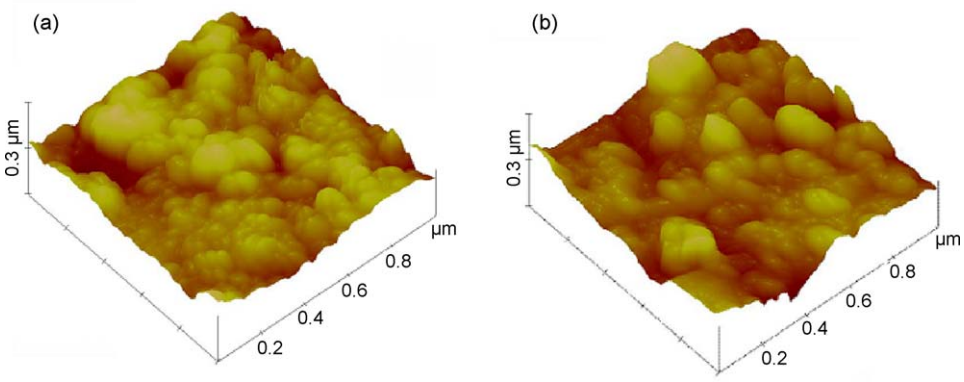

Fig. 4. AFM images of $CoWO_4$ deposited on glass substrates at (a) 350 and (b) 450 °C.

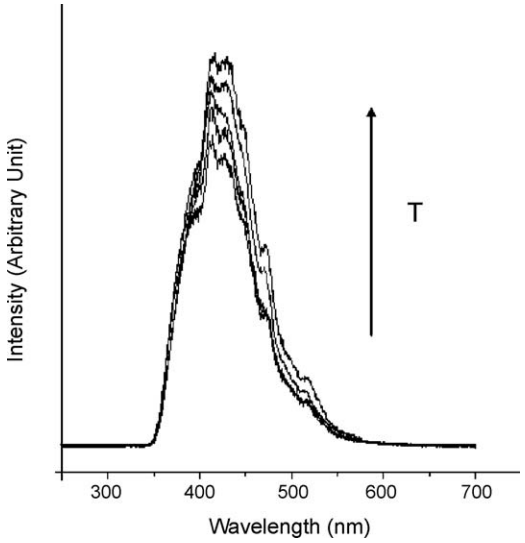

Fig. 5. PL spectra of $CoWO_4$ nano-particles produced at 250, 300, 350, 400 and 450 °C.

4. Conclusion

$CoWO_4$ nano-particles were successfully produced by spray pyrolysis at 250–450 °C. The products are pure phase with wolframite structure. They are composed of a number of nano-particles with their crystallographic planes aligning in a systematic array. Particle sizes and roughness increased with the increase in test temperature, due to the growth process. The particle sizes at different temperatures fitted very well with the Arrhenius-type equation. Vibrations of atoms provided evidence of the wolframite structure, corresponding to the product phase. PL emission shows the narrow central peaks of the same spectral region at 411–419 nm.

Acknowledgement

We are extremely grateful to the Thailand Research Fund for supporting the research.

References

[1] S.H. Yoon, D.W. Kim, S.Y. Cho, K.S. Hong, J. Eur. Ceram. Soc. 26 (2006) 2051–2054.
[2] J.T. Kloprogge, M.L. Weier, L.V. Duong, R.L. Frost, Mater. Chem. Phys. 88 (2004) 438–443.
[3] S.H. Yu, B. Liu, M.S. Mo, J.H. Huang, X.M. Liu, Y.T. Qian, Adv. Funct. Mater. 13 (2003) 639–647.
[4] R. Dafinova, K. Papazova, A. Bojinova, J. Mater. Sci. Lett. 17 (1998) 237–239.
[5] A. Golubović, R. Gajić, Z. Dohčević-Mitrović, S. Nikolić, J. Alloys Compd. 415 (2006) 16–22.
[6] X.C. Song, E. Yang, R. Ma, H.F. Chen, Y. Zhao, J. Nanopart. Res. 10 (2008) 709–713.
[7] T. Thongtem, A. Phuruangrat, S. Thongtem, Curr. Appl. Phys. 8 (2008) 189–197.
[8] H. Fu, C. Pan, L. Zhang, Y. Zhu, Mater. Res. Bull. 42 (2007) 696–706.
[9] L. Zhen, W.S. Wang, C.Y. Xu, W.Z. Shao, L.C. Qin, Mater. Lett. 62 (2008) 1740–1742.
[10] T. You, G. Cao, X. Song, C. Fan, W. Zhao, Z. Yin, S. Sun, Mater. Lett. 62 (2008) 1169–1172.
[11] T. Thongtem, A. Phuruangrat, S. Thongtem, Appl. Surf. Sci. 254 (2008) 7581–7585.
[12] Powder Diffract. File, JCPDS Internat. Centre Diffract. Data, PA 19073-3273, U.S.A., 2001.
[13] S.L. González-Cortés, T.C. Xiao, P.M.F.J. Costa, S.M.A. Rodulfo-Baechler, M.L.H. Green, J. Mol. Catal. A 238 (2005) 127–134.
[14] Scion Image, Scion Corp., 82 Worman's Mill Ct., Suite H, Frederick, MD 21701, 1997–2005.
[15] S. Thongtem, C. Boonruang, T. Thongtem, M. McNallan, Surf. Interface. Anal. 37 (2005) 765–769.
[16] Y. Zhang, N.A.W. Holzwarth, R.T. Williams, Phys. Rev. B 57 (1998) 12738–12750.
[17] M.J. Treadaway, R.C. Powell, J. Chem. Phys. 61 (1974) 4003–4011.
[18] V.B. Mikhailik, I.K. Bailiff, H. Kraus, P.A. Rodnyi, J. Ninkovic, Radiat. Meas. 38 (2004) 585–588.
[19] V. Pankratov, L. Grigorjeva, D. Millers, S. Chernov, A.S. Voloshinovskii, J. Lumin. 94–95 (2001) 427–432.